Acta Chemica Scandinavica, 1993: 47: 1154–1161
Printed in Belgium – all rights reserved

ACTA
CHEMICA SCANDINAVICA
ISSN 0904–213X

Magnetism, Spectroscopy and Structure of Tri-μ-hydroxobis{[*N,N′, N″*-trimethyl-1,1,1-tris(aminomethyl)ethane]chromium(III)} Chloride Tetrahydrate

Jørgen Glerup,[a,*] Sine Larsen[b] and Høgni Weihe[a]

[a]Chemical Laboratory I and [b]Chemical Laboratory IV, Department of Chemistry, H. C. Ørsted Institute, University of Copenhagen, Universitetsparken 5, DK-2100 København Ø, Denmark

Glerup, J., Larsen, S. and Weihe, H. 1993. Magnetism, Spectroscopy and Structure of Tri-μ-hydroxobis{[*N, N′, N″*-trimethyl-1, 1, 1-tris(aminomethyl) ethane]-chromium(III)} Chloride Tetrahydrate. – Acta Chem. Scand. 47: 1154–1161. © Acta Chemica Scandinavica 1993.

A new trihydroxo bridged chromium cation $[(Me_3\text{-tame})Cr(OH)_3Cr(Me_3\text{-tame})]^{3+}$, where Me_3-tame is [*N,N′,N″*-trimethyl-1,1,1-trisaminomethyl)-ethane], has been isolated as several salts. The structure of the cation isolated as a chloride tetrahydrate was determined from low-temperature X-ray data. This compound crystallizes in the monoclinic space group $P2_1/n$ with $a = 9.674(3)$, $b = 13.775(3)$, $c = 22.947(4)$ Å, $\beta = 102.50(2)°$ and $Z = 4$. Using 16 027 observed reflections the structure was refined to $R = 0.034$ and $R_w = 0.047$. The symmetry of the cation in the cloride salt is close to C_{3h} with a Cr–Cr distance of 2.6359(3) Å. The temperature-dependent magnetic susceptibility showed that the two chromium ions in the dimeric unit are antiferromagnetically coupled with a triplet–singlet seperation of 147 cm^{-1}. X-Band EPR spectra of a crystalline powder of the chloride salt showed lines which could be interpreted as transitions within the quintet and triplet state. Good estimates of the monomeric spin Hamiltonian parameters could be obtained by recording EPR spectra of the analogous Co–Co triol (or Cr–Cr triol) contamined with 1% of the Cr–Co triol. The EPR spectra were simulated with the parameters $D_1 = D_2 = 0.80$ cm^{-1}, $E_1 = E_2 = -0.0085$ cm^{-1}, $D_e = 0.0194$ cm^{-1} and $E_c = 0.0049$ cm^{-1}.

In recent years several chromium(III) triols [tri-μ-hydroxobischromium(III) complexes] have been prepared with different amines, e.g. 1,4,7-trimethyl-1,4,7-triazacyclononane,[1] 1,5,9-triazacyclododecane[2] and ammonia.[3] We and others have unsuccessfully tried to prepare chromium(III) triols with ligands like 1,4,7-triazacyclononane,[4] 1,1,1-tris(aminomethyl)ethane and *cis–cis*-1,3,5-cyclohexanetriamine. Recently we have prepared not a triol but a adamantane-like tetranuclear chromium(III) complex[5] with the last mentioned amine. From a comparison of the structures mentioned above one could get the idea that steric hindrance is an important aspect in the formation of triols, or more precisely that bulky groups in the vicinity of the bridging hydroxo groups impede dissociation of the formed triols to *cis*-diols. Following these ideas we will describe the successful preparation of a new triol with the ligand [*N,N′,N″*-trimethyl-1,1,1-tris(aminomethyl)ethane] (Me_3-tame). Contrary to the abovementioned ligands, this ligand is easy to prepare, but has the disadvantage that several isomers of the mononuclear as well as the dinuclinear complexes are possible.

Results and discussion

Synthesis. According to the simple reaction schemes (I)

$$Cr(thf)_3Cl_3 + Me_3\text{-tame} \xrightarrow{thf} Cr(Me_3\text{-tame})Cl_3 + 3\ thf \quad (I)$$

$$2Cr(Me_3\text{-tame})Cl_3 + 3\ OH^- \xrightarrow{H_2O} [(Me_3\text{-tame})Cr(OH)_3Cr(Me_3\text{-tame})]Cl_3 \cdot 4H_2O + 3Cl^- \quad (II)$$

and (II) it is possible to isolate the tri-μ-hydroxo bridged chromium dimer as a chloride tetrahydrate. The first reaction proceeded quantitatively, but the yields in the last

* To whom correspondence should be addressed.

step never exceeded 50%. We tried, but unsuccesfully, to improve the yields in the last step by changing the anion to bromide. This was done by using $Cr(thf)_3Br_3$ instead of $Cr(thf)_3Cl_3$. The reason for these low yields must then have another explanation. The presence of the methyl groups on the nitrogen atoms causes a total number of four possible isomers of $Cr(Me_3\text{-tame})Cl_3$, the four isomers being grouped into two sets of two enantiomers. These four isomers are distinguished by the directions of the methyl groups relative to the (pseudo) three-fold axis of $Cr(Me_3\text{-tame})Cl_3$. If all the coordinated nitrogen atoms have identical chirality, i.e. if the methyl groups are pointing in a clockwise or counter-clockwise direction with respect to this axis, the axis is a true three-fold axis. It could be expected that the condensation in the second step probably produces numerous different species, including possibly *cis* and *trans* diols, two triol isomers, one with C_{3h} symmetry and one with D_3 symmetry, and oligomers of higher nuclearity in the solution, but only the triol isomer with idealized C_{3h} symmetry crystallizes from the solution. However, Andersen *et al.*[6] have shown that the isomer with idealized D_3 symmetry can be isolated by a rather different route.

Structure. The crystal structure determination confirms that the cation is a tri-μ-hydroxo bridged dichromium cation with the two Me_3-tame ligands facially coordinating. A thermal ellipsoid plot of the cation is shown in Fig. 1, which also gives the numbering scheme used. The bond lengths and angles in the coordination sphere of chromium are listed in Table 1. The Cr–O distances display some small differences that can be related to differences in the hydrogen bonding of the bridging hydroxo groups (*vide infra*). Apart from this, the overall symmetry of the cation is close to C_{3h}. The Cr1–Cr2 distance is 2.6359(3) and is similar to those observed in other chromium(III) triols. Similarly, the averaged Cr–O and Cr–N distances and the averaged O–Cr–O and Cr–O–Cr angles of 1.9700(10) Å, 2.0869(9) Å, 80.12° and 84.01°, respectively, are consistent with those in other related systems.[1–3]

Only a few complexes of tame and Me_3-tame have been characterized structually. The bond lengths and angles in the two Me_3-tame ligands are listed in Table 2. The two independent ligands are remarkably alike, not only with

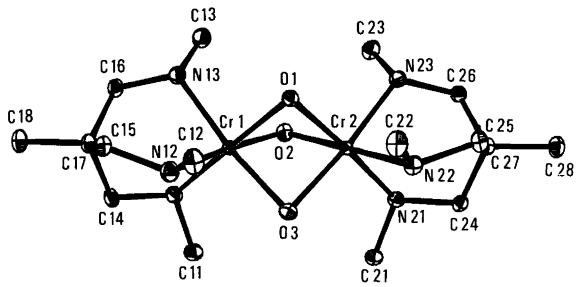

Fig. 1. Thermal ellipsoid plot of the ion $[(Me_3\text{-tame})Cr(OH)_3Cr(Me_3\text{-tame})]^{3+}$.

Table 1. Bond lengths (in Å) and angles (in °) in the coordination sphere of chromium(III).

Atoms	*i* = 1	*i* = 2	*i* = 3
Bond lengths			
Cr*i*–O1	1.9654(11)	1.9647(10)	
Cr*i*–O2	1.9827(11)	1.9876(10)	
Cr*i*–O3	1.9523(10)	1.9644(9)	
Cr*i*–N*i*1	2.0909(11)	2.0930(11)	
Cr*i*–N*i*2	2.0730(11)	2.0886(11)	
Cr*i*–N*i*3	2.0796(11)	2.0961(11)	
Angles			
O1–Cr*i*–O2	80.08(4)	79.97(4)	
O2–Cr*i*–O3	79.76(4)	79.36(4)	
O3–Cr*i*–O1	80.92(4)	80.65(4)	
N*i*1–Cr*i*–N*i*2	86.62(4)	88.04(4)	
N*i*2–Cr*i*–N*i*3	89.05(4)	89.28(4)	
N*i*3–Cr*i*–N*i*1	87.55(4)	86.04(4)	
Cr1–O*i*–Cr2	84.24(4)	83.19(4)	84.60(4)
Cr1–Cr2–O*i*	47.89(3)	48.32(3)	47.56(3)
Cr2–Cr1–O*i*	47.87(3)	48.49(3)	47.92(3)
N11–Cr1–O*i*	175.90(5)	95.81(5)	98.47(5)
N12–Cr1–O*i*	97.45(5)	174.13(4)	94.68(5)
N13–Cr1–O*i*	92.84(5)	96.36(5)	173.08(5)
N21–Cr2–O*i*	176.32(5)	98.02(4)	95.98(5)
N22–Cr2–O*i*	93.78(4)	173.09(5)	96.86(5)
N23–Cr2–O*i*	97.17(4)	94.41(4)	173.59(4)

Table 2. Bond lengths (in Å) and angles (in °) of the ligand.

Atoms	*i* = 1	*i* = 2
Bond lengths		
C*i*8–C*i*7	1.534(2)	1.534(2)
C*i*7–C*i*6	1.532(2)	1.530(2)
C*i*7–C*i*5	1.537(2)	1.537(2)
C*i*7–C*i*4	1.534(2)	1.537(2)
C*i*6–N*i*3	1.489(2)	1.493(2)
C*i*5–N*i*2	1.492(2)	1.490(2)
C*i*4–N*i*1	1.500(2)	1.497(2)
N*i*1–C*i*1	1.488(2)	1.489(2)
N*i*2–C*i*2	1.489(2)	1.489(2)
N*i*3–C*i*3	1.477(2)	1.486(2)
Angles		
C*i*8–C*i*7–C*i*6	107.7(1)	108.4(1)
C*i*8–C*i*7–C*i*5	108.4(1)	108.1(1)
C*i*8–C*i*7–C*i*4	108.2(1)	107.9(1)
C*i*6–C*i*7–C*i*5	110.6(1)	110.3(1)
C*i*5–C*i*7–C*i*4	110.8(1)	110.9(1)
C*i*4–C*i*7–C*i*6	111.0(1)	111.1(1)
C*i*7–C*i*6–N*i*3	113.3(1)	113.7(1)
C*i*7–C*i*5–N*i*2	112.2(1)	112.2(1)
C*i*7–C*i*4–N*i*1	113.4(1)	113.8(1)
C*i*6–N*i*3–C*i*3	110.5(1)	109.4(1)
C*i*5–N*i*2–C*i*2	109.8(1)	108.7(1)
C*i*4–N*i*1–C*i*1	109.0(1)	109.4(1)
Torsion angles		
N*i*1–C*i*4–C*i*7–C*i*8	161.7(1)	−159.8(1)
N*i*2–C*i*5–C*i*7–C*i*8	160.0(1)	−158.5(1)
N*i*3–C*i*6–C*i*7–C*i*8	162.7(1)	−164.9(1)
C*i*1–N*i*1–C*i*4–C*i*7	159.9(1)	−163.8(1)
C*i*2–N*i*2–C*i*5–C*i*7	167.9(1)	−166.0(1)
C*i*3–N*i*3–C*i*6–C*i*7	162.9(1)	−158.0(1)

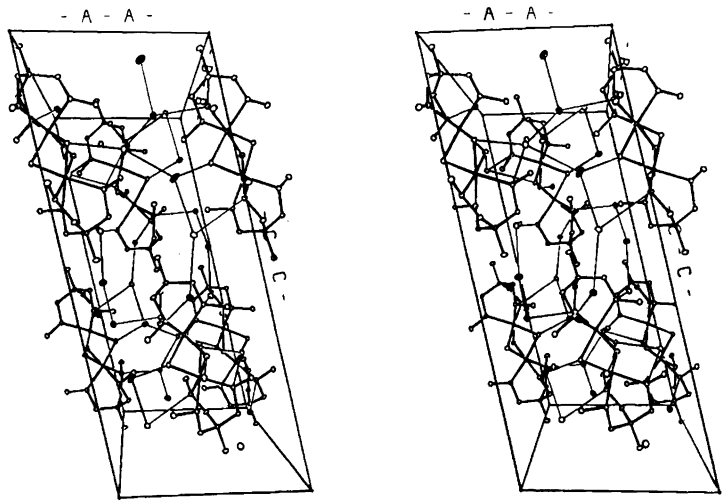

Fig. 2. ORTEP stereoview showing the packing in $[(Me_3\text{-tame})Cr(OH)_3Cr(Me_3\text{-tame})]Cl_3 \cdot 4H_2O$. The hydrogen bonds are indicated with thin lines.

respect to bond lengths and angles but also in their conformation. They are almost true mirror images of each other.

The packing in the crystal is strongly influenced by hydrogen bonding. They are illustrated in the stereo pair in Fig. 2 and their geometry in Table 3. Two of the hydroxo groups are hydrogen-bonded to chloride ion Cl2, whereas the third hydroxo group is acting as a donor towards one of the water molecules. It should be noted that the Cr–O distance is shorter for this particular hydroxo group. As shown in Fig. 2, the hydrogen bond that links the cations, the chloride ions and the water molecules leads to different environments for the two halves of the complex cation.

Table 3. Hydrogen bonds.

Atoms	H–A	D–H–A	D–A
O1–HO1 ··· C12[a]	2.59(2)	145(2)	3.2399(9)
O2–HO2 ··· C12	2.31(2)	171(2)	3.110(1)
O3–HO3 ··· OW3[b]	2.35(2)	99(2)	2.655(2)
OW1–H1W1 ··· OW4	2.02(2)	170(2)	2.765(2)
OW1–H2W1 ··· C12[a]	2.40(2)	179(2)	3.200(1)
OW2–H1W2 ··· C13[e]	2.40(2)	176(2)	3.226(1)
OW2–H2W2 ··· C13[d]	2.55(2)	175(2)	3.188(1)
OW3–H1W3 ··· C12[a]	2.46(2)	175(2)	3.148(1)
OW3–H2W3 ··· C13	2.24(2)	166(2)	3.110(2)
OW4–H1W4 ··· C11[c]	2.35(2)	172(2)	3.150(2)
OW4–H2W4 ··· C11[a]	2.37(2)	166(2)	3.157(2)
N11–HN11 ··· OW2	2.11(2)	149(2)	2.979(2)
N12–HN12 ··· OW1	1.96(2)	160(2)	2.900(2)
N13–HN13 ··· C11[a]	2.21(2)	175(2)	3.212(1)
N21–HN21 ··· C11	2.47(2)	145(2)	3.314(1)
N22–HN22 ··· C13[b]	2.39(2)	159(2)	3.268(1)
N23–HN23 ··· C12[a]	2.37(2)	160(2)	3.227(1)

[a] (−2, 1, −1, 0). [b] (1, 1, 0, 0). [c] (2, −1, 0, −1). [d] (−2, 1, 0, 0). [e] (2, 0, 0, −1).

UV–VIS spectrum. A UV–VIS spectrum of the title compound is shown in Fig. 3. The normal spin-allowed d–d transitions have the (λ_{max}/nm, ε_{max}/cm^{-1}mol^{-1}l)-values (511, 111.7) and (379, 61.7), corresponding to the monomer exited-state energies of $^4T_2(t_2^2e)$ and $^4T_1(t_2^2e)$ of, respectively, 18 148 and 26 385 cm^{-1} above the ground state. Here all states will be labeled by pure octahedral transformation properties together with the strong-field electron configuration. Fig. 4 present the spectrum of the cation $[Cr(Me_3\text{-tame})(OH_2)_3]^{3+}$ obtained by hydrolyzation of the triol in 6 M perchloric acid. It is remarkable that the abovementioned two transitions have the same energy and almost the same intensity per chromium atom, even though in the first case the ligands are bridging hydroxo groups and in the latter case the ligands are coordinated water molecules.

The six weak maxima in Fig. 3 with (λ_{max}, ε_{max})-values (691, 1.9), (681, 2.5), (659, 2.0), (626, 2.4), (620, 3.4) and (613, 3.2) are due to one-center–one-electron transitions

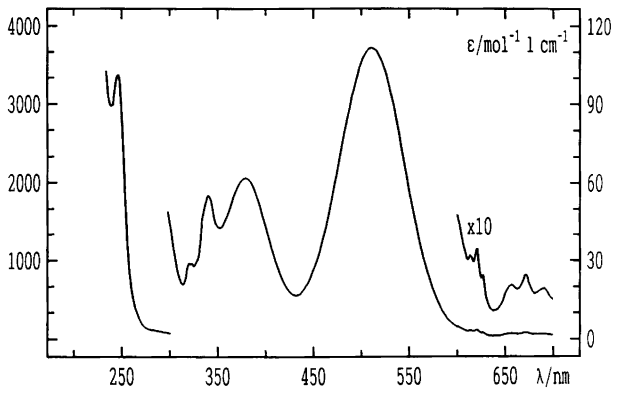

Fig. 3. UV–VIS spectrum of $[(Me_3\text{-tame})Cr(OH)_3Cr(Me_3\text{-tame})]^{3+}$ in water.

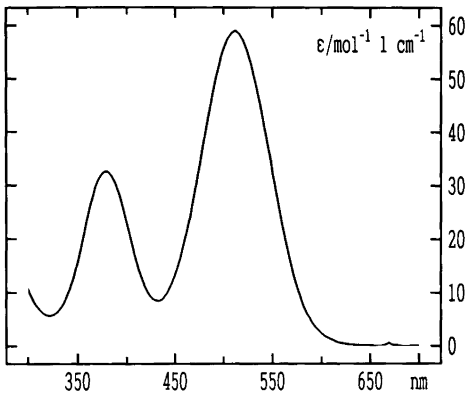

Fig. 4. UV–VIS spectrum of $[Cr(Me_3\text{-tame})(OH_2)_3]^{3+}$ in perchloric acid.

to excited states lying in the energy interval from 14 472 to 16 313 cm^{-1} above the ground state. In monomeric chromium(III) complexes the observed bands in this region are spin-forbidden transitions. Besides the spin-forbidden transitions in dimeric chromium(III) complexes allowed transitions emerge as a result of the antiferromagnetic coupling. These transitions can be characterized as hot bands from the triplet and quintet states of the ground-state manifold $(^4A_2, t_2^3)(^4A_2, t_2^3)$ to the triplets and quintets of the excited states $(^4A_2, t_2^3)(^2E, t_2^3)$ and $(^4A_2, t_2^3)(^2T_1, t_2^3)$. The maxima and shoulders (sh) (340, 55.4), $(335, 48.2)_{sh}$, $(327, 28.8)_{sh}$, (323, 28.9) and (321, 28.9) are due to transitions, which in the strong-field limit are characterized as two-center–two-electron transitions from the singlet and triplet in the ground-state manifold to the singlet and triplets of $(^2E,t_2^3)(^2E,t_2^3)$, $(^2E,t_2^3)(^2T_1,t_2^3)$ and $(^2T_1, t_2^3)(^2T_1, t_2^3)$. It should be emphasized here that the energies of these states, lying in the energy interval from 29 412 to 31 153 cm^{-1} relative to the ground state, have, as expected, almost twice the energies of the one-electron–one-center excited states mentioned above. The high-intensity band (247, 3376) is assigned to the Laporte-allowed charge-transfer transition where one electron is moved from one chromium center to the other chromium center.[7] The energy, E_{CT}, of the charge transfer state is 40 486 cm^{-1}. This interpretation, together with the J-value obtained from the magnetic susceptibility measurements (*vide infra*), enables one to calculate the π-parameter for the hydroxo ligand $\Delta_{\pi OH}$ from eqn. (1).

$$E_{septet} - E_{singlet} = \frac{(-\sqrt{3}/2\,\Delta_{\pi OH})^2}{E_{CT}} = 6J = 882\ cm^{-1} \qquad (1)$$

The value obtained for $\Delta_{\pi OH} = 6.900\ cm^{-1}$ is in good agreement with the value we have obtained elsewhere,[8] even though this calculation does not consider the possibility for a direct metal–metal interaction.[9]

Magnetic susceptibility. In Fig. 5 are shown the magnetic susceptibility (cgs units, cm^3/mol) and the effective magnetic moment. The susceptibility at room temperature is 4×10^{-3} and decreases to 5×10^{-4} at 15 K and increases again on further cooling. This is typical behaviour for a dinuclear chromium(III) complex with a considerable antiferromagnetic coupling contaminated with a small amount of a paramagnetic impurity.

The temperature dependence of the magnetic susceptibility was approximated by eqn. (2) by minimization of expression (3) within the framework of nonlinear regression analysis.

$$\chi'_{mol,calc} = -\frac{N}{H}\frac{\sum_i \frac{\partial E_i}{\partial H}\exp(-E_i/kT)}{\sum_i \exp(-E_i/kT)} + K + \frac{C}{T} \qquad (2)$$

$$\sum_T \frac{(\chi_{exp} - \chi_{calc})^2}{\sigma^2(\chi') + \left(\frac{\partial \chi}{\partial T}\right)^2 \sigma^2(T)} \qquad (3)$$

$\sigma^2(T)$ and $\sigma^2(\chi)$ are the estimated standard deviations on the measured magnetic susceptibility and temperature, respectively. In eqn. (2) C/T accounts for paramagnetic impurities, while K accounts for temperature paramagnetism and minor deviations in the correction for diamagnetism which was made using Pascal's constants. The energies E_i of the 16 components of the ground-state manifold were obtained as the eigenvalues of the isotropic spin Hamiltonian (4), where we naturally have assumed

$$\boldsymbol{H} = g_1\mu_B S_1 \cdot H + g_2\mu_B S_2 \cdot H + JS_1 \cdot S_2 \qquad (4)$$

that the g-values for the two chromium ions are identical. The parameters obtained were $g = 2.00$ and $J = 147\ cm^{-1}$.

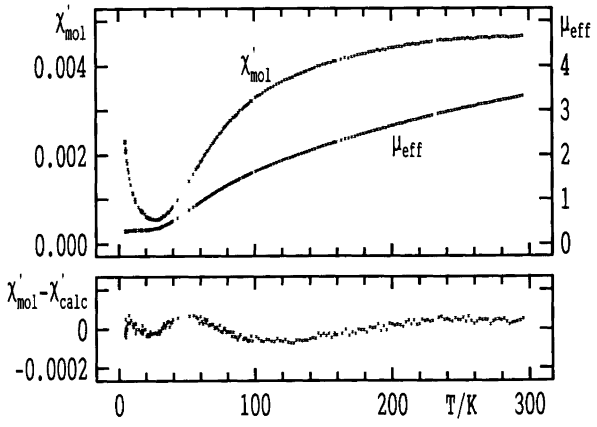

Fig. 5. Magnetic susceptibility (cgs units, cm^3/mol) and effective magnetic moment of the triol.

EPR spectra. Measuring EPR spectra of crystalline solids, including powder samples as well as single crystals, generally requires that the paramagnetic species has been diluted in a diamagnetic host, e.g. dilution of a chromium(III) compound in an isomorphous cobalt(III) complex. This magnetic dilution can also be achieved if the compound under consideration itself has a sufficient inherent antiferromagnetic coupling, as is the case with many dimeric chromium(III) compounds. Our goal with the EPR measurements of this chromium(III) triol was to determine all the parameters in the spin Hamiltonian (*vide infra*) used for interpretation of di- and polynuclear complexes containing paramagnetic ions. The term in J is by far the most dominant term in the operator. This gives in our case a singlet ground state and triplet, quintet and septet excited states. Since all four states are well separated, the EPR spectrum is expected to be composed of a simple sum of spectra from the three excited states, each weighted with its appropriate Boltzmann factor. We[10,11] and others[12] have shown that the absolute values of the anisotropic exchange parameters, D_e and E_e, can be determined with great accuracy from the zero field splitting (zfs) of the quintet spectrum alone, because the monomeric parameters, D_1, D_2, E_1 and E_2, only exert second-order effects on the zfs of the quintet. The absolute values of the zfs parameters in the triplet and septet states can, on the other hand, be approximated by certain linear combinations of the anisotropic exchange parameters and the monomeric parameters. Solving the equations thus introduced will always lead to ambiguities concerning both the signs and the magnitudes of the solutions. To circumvent these problems we therefore proceeded in another way. To get information about the monomeric zfs parameters we synthesized the mixed cobalt–chromium triol doped in the pure cobalt triol as well as in the pure chromium triol. In the first case when the mixed triol is diluted in the pure cobalt triol, the cobalt triol is a normal diamagnetic host. In the latter case the pure chromium triol behaves as a diamagnetic host at low temperatures, since only the singlet state is populated at sufficiently low temperature. While we are aware that the bond angles and bond lengths around the two metal ions are not necessecarily identical, the EPR spectrum of this mixed triol should at least give a clue about the sizes of the monomeric zfs parameters in the dimeric system.

An X-band spectrum of the undiluted title compound is shown in Fig. 6. This spectrum was recorded at 80 K. From the temperature variation of the intensities of the lines in the region from 0.25 to 0.45 T it could be shown that these lines are transitions within the quintet state, and for the two broad lines in the interval 0.75–1 T the temperature variation of the intensities shows that they can be assigned as transitions within the triplet state. Fig. 7 shows an X-band spectrum of the mixed triol diluted in the pure cobalt triol. The spectrum of the mixed triol diluted in the pure chromium triol (not shown here) is almost identical to this spectrum. The only differences are minor variations in the pattern of lines at 1.2 T.

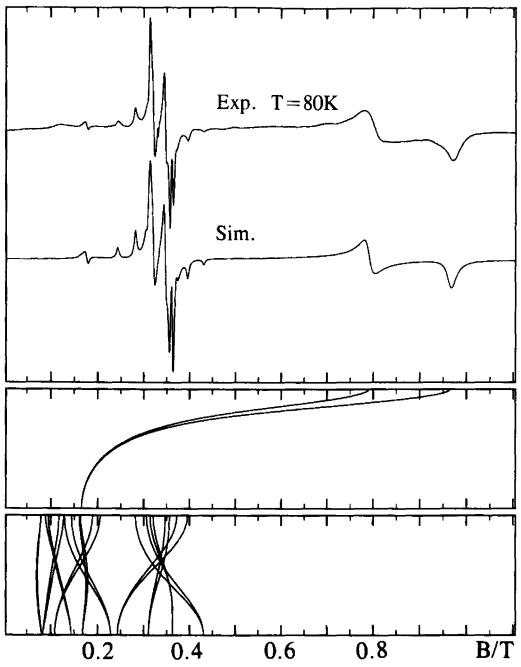

Fig. 6. Upper curve shows the X-band EPR spectrum of the triol at 80 K measured on a crystalline powder. Below is the simulated spectrum, which is a sum of the spectrum from the quintet state (0.2–0.4 T) and the spectrum from the triplet state (0.75–1 T), each weighted by the appropriate Boltzmann factor. The two lower graphs give a representation of the resonance condition within the triplet state and within the quintet state as a function of the orientation of the magnetic field relative to the molecular z-axis, respectively.

The similarities of these two spectra demonstrate that this is really the EPR spectrum of the genuine mixed cobalt–chromium triol.

Simulation of EPR spectra. The EPR spectra of the chromium triol were interpreted in terms of the usual spin Hamiltonian operator applied to dimeric systems, eqn. (4), where $\boldsymbol{H}_{ex}$ and $\boldsymbol{H}_1$ are given by eqns. (5) and (6), respectively, and a similar term defines $\boldsymbol{H}_2$. All the

$$\boldsymbol{H} = \boldsymbol{H}_1 + \boldsymbol{H}_2 + \boldsymbol{H}_{ex} \tag{4}$$

$$\boldsymbol{H}_{ex} = J\boldsymbol{S}_1 \cdot \boldsymbol{S}_2 + D_e[2\boldsymbol{S}_{1z}\boldsymbol{S}_{2z} - \boldsymbol{S}_{1x}\boldsymbol{S}_{2x} - \boldsymbol{S}_{1y}\boldsymbol{S}_{2y}] + E_e[\boldsymbol{S}_{1x}\boldsymbol{S}_{2x} - \boldsymbol{S}_{1y}\boldsymbol{S}_{2y}] \tag{5}$$

$$\boldsymbol{H}_1 = \mu_B[g_{1x}\boldsymbol{S}_{1x}H_x + g_{1y}\boldsymbol{S}_{1y}H_y + g_{1z}\boldsymbol{S}_{1z}H_z] + D_1(\boldsymbol{S}_{1z}^2 - \tfrac{1}{3}S_1(S_1+1)] + E_1[\boldsymbol{S}_{1x}^2 - \boldsymbol{S}_{1y}^2] \tag{6}$$

parameters have their usual meanings. We have previously discussed the simulation of EPR spectra for dinuclear chromium(III) complexes.[10,11]

The spectra of the mixed triol could be interpreted by use of $\boldsymbol{H}_1$. The spectrum in Fig. 7 clearly shows two slightly different chromium ions. This is in full accordance with the crystal structure, which shows that the two

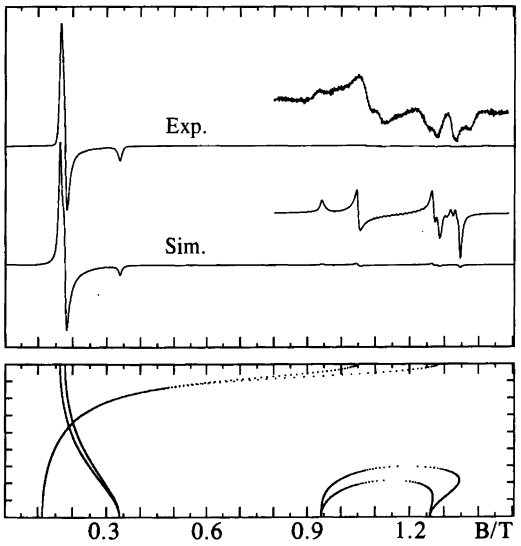

Fig. 7. X-Band EPR spectrum of the mixed chromium–cobalt triol diluted on the cobalt–cobalt triol. Below is shown the simulated spectrum together with a graphic representation of the resonance condition as a function of the magnetic field relative to the molecular *z*-axis.

chromium ions in the dimeric unit are distinguishable. Therefore this spectrum had to be interpreted as a sum of two spectra with slightly different spin Hamiltonian parameters. The spectrum in Fig. 7 was simulated with the following parameters for site 1: $D_1 = 1.045\ cm^{-1}$, $E_1 = 0.034\ cm^{-1}$, $g_{1x} = g_{1y} = 1.985$ and $g_{1z} = 1.990$. The other site could be represented with the parameters $D_2 = 1.040\ cm^{-1}$, $E_2 = 0.020\ cm^{-1}$ and the same *g*-values as those for site 1. The interpretation of the powder spectrum is greatly simplified by the graphic representation of the angular dependence of the resonance magnetic fields (lower part of Fig. 7). In this figure only site 1 is represented.

Comparison of the relatively large zfs found for chromium in this mixed triol to the very small zfs found in, for instance, the structurally related[13] *fac*-$Cr(NH_3)_3(H_2O)_3^{3+}$, with holohedrized symmetry of O_h, suggests that it must be the geometrical distortion in the bridging arrangement which produces the zfs of the magnitude observed. In this context it can be mentioned that large zfs are generally observed in trigonally distorted chromium(III) complexes. In tetragonal complexes the main contribution to the zfs is usually attributed to the combined effect of spin–orbit coupling and ligand fields of tetragonal symmetry[14], since there exists a non-diagonal spin–orbit coupling matrix element between the ground state and the $^4T_2(t_2^2e)$ excited state, and because the $^4T_2$ is split in first order in the tetragonal field. In trigonally distorted d^3 complexes there is, in addition to the above-mentioned spin–orbit coupling matrix element, a nondiagonal ligand field matrix element connecting the ground-state term $^4A_2$ to one excited-state term, namely the $^4A_2$ component of the octahedral $^4T_1(t_2^2e)$ term. However, in the AOM formalism[15] this non-diagonal matrix element can be shown to vanish, if all six ligands are located at the vertices of an octahedron, i.e. holohedrized symmetry of O_h. The ligand field felt by the three unpaired electrons around chromium in the mixed triol is strongly anisotropic, since the mean value of the Cr–Cr–O angles is 48.0°, compared to arccos $(1/\sqrt{3})$ (= 54.7°) if the holohedrized symmetry were O_h. From this discussion we conclude that the main contribution to the zfs in trigonal symmetry is the distortion of the ligand positions away from octahedral positions.

Since the Co–O bonds[16] are somewhat shorter than the Cr–O bonds, and the Co–O–Co angles are equal to the Cr–O–Cr angles, the coordination geometry around chromium is expected to be more distorted in the mixed triol than in the pure chromium triol. This was also found experimentally (*vide infra*).

The spectrum of the chromium triol was interpreted in terms of the operator (4). By computation of a number of spectra only including the parameters J, D_e and E_e, using the J-value found from the magnetic susceptibility measurement, we find by a trial and error approach that $|D_e| = 0.0194\ cm^{-1}$ and $|E_e| = 0.0049\ cm^{-1}$. All four sign combinations did, as expected, give a fair reproduction of the quintet spectrum, with the major discrepency being too big a distance between the two lines with minima at 0.3574 and 0.3649 T (Fig. 6). This discrepency was cured by introducing the monomeric zfs in the calculation. Owing to the non-diagonal matrix element between the singlet and the $M_S = 0$ component of the quintet (7) it is

$$\langle 20\,|\boldsymbol{H}|\,00\rangle = -3D_e + D_1 + D_2 \qquad (7)$$

possible to determine the sign of D_e to be positive, since this choice results in a decreased distance between the two abovementioned lines. However, the best fit was obtained using $D_1 = D_2 = 0.80\ cm^{-1}$ and not the value found for the mixed triol as discussed above. This value gives a virtually perfect triplet spectrum as shown in Fig. 6. It should be mentioned that there is another solution with $D_1 = D_2 = -0.715\ cm^{-1}$. We have chosen the value $0.80\ cm^{-1}$, since this value is numerically closer to the zfs found in the mixed complex. The bandshapes were approximated with Lorentzian curves; a half-width of 7 mT was used for the quintet spectrum and we were forced to use a half-width of 22 mT for the triplet spectrum.

The conclusion from our experiment that D_e is positive is contrary to the general belief that the sign of D_e should be negative, since the main contribution to this term is assumed to be the magnetic dipole–dipole interaction.[17]

Experimental

Materials. The ligand was prepared according to the method of Kosowsky and Bailar.[18] $Cr(thf)_3Cl_3$ was prepared as described by Herwig and Zeiss.[19] All other chemicals were at least of reagent grade and were used without further purification.

Preparations

Tri-μ-hydroxobis[(Me$_3$-tame)chromium(III)] chloride tetrahydrate. [(Me$_3$-tame)Cr(OH)$_3$Cr(Me$_3$-tame)]Cl$_4$ · 4H$_2$O. 20 g (53 mmol) of Cr(thf)$_3$Cl$_3$ were dissolved in boiling thf (200 ml). 9 g of Me$_3$-tame dissolved in 40 ml thf were added slowly. The green precipitate [(Me$_3$-tame)CrCl$_3$] was filtered of and washed with boiling thf. Yield: 17 g (quantitative). This product is hygroscopic and was used without further purification.

10 g [(Me$_3$-tame)CrCl$_3$] (31 mmol) and 1.95 g LiOH · H$_2$O (46 mmol) were dissolved in 30 ml of water. This solution was left at 70°C for 8 h. After cooling, the red crystals were filtered of and washed with ethanol (96%) and diethylether. Yield: 4.2 g (42%).

Anal. Calc. for title compound Cr: 15.95%; C: 29.48%; H: 8.19%; N: 12.89%; Cl: 16.31%; Found Cr: 15.93%; C: 29.58%; H: 8.62%; N: 12.94%; Cl: 16.00%.

Crystals of X-ray quality were grown by evaporation of a saturated aqueous solution of the crude product at room temperature.

Tri-μ-hydroxobis[(Me$_3$-tame)cobalt(III)] chloride tetrahydrate. [(Me$_3$-tame)Co(OH)$_3$Co(Me$_3$-tame)]Cl$_4$ · 4H$_2$O. To 6.07 g Na$_3$[Co(NO$_2$)$_6$] (15 mmol) in 30 ml of boiling water was slowly added 2.38 g Me$_3$-tame dissolved in 10 ml water. The brown–orange product, Co(Me$_3$-tame)(NO$_2$)$_3$, was removed by filtration and then washed with water, ethanol and diethyl ether. Insolubility prevented purification of this product, and it was used as synthesized. 2.05 g Co(Me$_3$-tame)(NO$_2$)$_3$ were boiled in 6 M HCl for 1 h, giving a green solution. This solution was evaporated to dryness in a rotavapor. Yield: 1.70 g of green Co(Me$_3$-tame)Cl$_3$. The Co-triol was synthesized as described above.

Tri-μ-hydroxo[(Me$_3$-tame)chromium(III)(Me$_3$-tame)-cobalt(III)] chloride tetrahydrate. ([Me$_3$-tame)Cr(OH)$_3$-Co(Me$_3$-tame)]Cl$_4$ · 4H$_2$O. It was not attempted to synthesize this mixed dimer in its pure form, but it was prepared as a minor constituent in the Co–Co dimer and in the Cr–Cr dimer. In the first case we used 99% Co(Me$_3$-tame)Cl$_3$ and 1% Cr(Me$_3$tame)Cl$_3$ and performed the condensation in the manner described above. The chromium/cobalt ratio in the product was not analyzed but was assumed to be 1%. Cr–Co triol diluted into the pure Cr–Cr triol was synthesized analogously using 99% Cr(Me$_3$-tame)Cl$_3$ and 1% Co(Me$_3$-tame)Cl$_3$.

X-ray crystallography. Tri-μ-hydroxobis[(Me$_3$-tame)-chromium(III)] chloride tetrahydrate crystallizes as red prisms with developed faces {001} and {110}. Weissenberg photographs showed that they belong to the monoclinic system. The space group is uniquely determined to be $P2_1/n$, a non-standard setting of $P2_1/c$.

A CAD4 diffractometer equipped with monochromatized Mo$K\alpha$ radiation was used for the data collection. The crystal was cooled to 110 K with an Enraf-Nonius gas-flow low-temperature device during the experiment. The unit-cell parameters were determined from least-squares refinement of the setting angles of 18 reflections with $16.5 < \theta < 22°$. Based on an analysis of reflection profiles the scan type and range were selected. The crystal data and a summary of the data reduction and refinement results are given in Table 4. The intensities of three standard reflections were measured every 10^4 s, and the orientation of the crystal was checked every 300 reflections. These measurements showed that no mis-setting or degradation of the crystal occured during the data collection. Data reduction included corrections for background, Lorentz polarization and absorbtion effects. The latter correction was performed by the Gaussian integration procedure. The transmission factors were in the range 0.779–0.858. Symmetry-related reflections were averaged. The positions of the two chromium atoms were deduced from the Patterson function. The remaining non-hydrogen atoms were localized in two successive Fourier calculations. The structure was refined by minimizing $\Sigma w(|F_o| - |F_c|)^2$. After anisotropic displacement parameters had been introduced the hydrogen atoms were found from a difference Fourier map. Their positional parameters were included in the refinement. Common isotropic displacement parameters for the hydrogen atoms of 2 Å^2 were introduced, since attempts to refine the displacement parameters gave a physically unrealistic value to one of the bridging hydroxo ion. The SDP-system[20] was employed for the crystallographic computations. The atomic scattering factors, including contribu-

Table 4. Crystal data and a summary of results from data reduction and structure refinement.

Formula	$Cr_2O_7N_6Cl_3C_{16}H_{53}$
Formula weight/g mol^{-1}	651.98
Space group	$P2_1/n$ (monoclinic)
Crystal size/mm	0.12 × 0.25 × 0.35
Temperature/T	110(1)
Radiation/Å	Mo$K\alpha$, 0.710 73
Cell parameters at 110 K	
a/Å	9.674(3)
b/Å	13.775(3)
c/Å	22.947(4)
β/°	102.50(2)
Z	4
Calculated density/g cm^{-3}	1.451
Linear absorption coefficient/cm^{-1}	10.233
Scan type	ω-2θ
Scan width Δθ/°	0.7 + 0.35 tan θ
Background	25% of full scan on both sides
Max. scan time/s	60
Max. specified $\sigma(I)/I$	0.01
θ range/°	1–38
Maximum and minimum h,k,l values	0 – 16, 0 – 23, −39 – 38
No. of unique data	16 030
Internal R-value from averaging	0.014
No. of contributing reflections, ($\|F\|^2 > 3\sigma\|F\|^2$)	10 604
No. of variables, m	466
Weights, w^{-1}	$\sigma_{cs}^2(F) + 0.0006\|F\|^2$
R	0.034
R_w	0.047
Max. shift/error	0.03
$S = \{\Sigma w \Delta F^2/(n-m)\}^{1/2}$	1.33

Table 5. Positional parameters and equivalent isotropic displacement parameters.

Atom	*x*	*y*	*z*	B_{iso}[a]
Cr1	0.95085(2)	0.18663(2)	0.18126(1)	0.775(3)
N13	0.7894(1)	0.18286(9)	0.10493(5)	1.18(2)
N11	1.0477(1)	0.29332(9)	0.13899(6)	1.22(2)
N12	1.0621(1)	0.08624(9)	0.14205(5)	1.22(2)
C13	0.6569(2)	0.2330(1)	0.10907(7)	1.71(3)
C12	1.0692(2)	−0.0144(1)	0.16620(7)	1.39(2)
C11	1.1736(2)	0.3400(1)	0.17764(7)	1.52(2)
C16	0.8307(2)	0.2078(1)	0.04787(6)	1.18(2)
C15	1.0254(2)	0.0834(1)	0.07550(6)	1.11(2)
C14	1.0848(2)	0.2623(1)	0.08164(6)	1.25(2)
C17	0.9856(2)	0.1841(1)	0.04815(6)	1.10(2)
C18	1.0018(2)	0.1826(1)	−0.01691(6)	1.50(2)
Cr2	0.91495(2)	0.18183(2)	0.29187(1)	0.738(3)
N21	0.9893(1)	0.27951(9)	0.36146(5)	1.08(2)
N22	0.9810(1)	0.06910(9)	0.35238(5)	1.12(2)
N23	0.7221(1)	0.18666(9)	0.31939(5)	1.09(2)
C21	1.1287(2)	0.3249(1)	0.36094(7)	1.43(2)
C22	0.9812(2)	−0.0299(1)	0.32637(7)	1.38(2)
C23	0.6147(2)	0.2542(1)	0.28515(7)	1.49(2)
C24	0.9918(2)	0.2387(1)	0.42214(6)	1.06(2)
C25	0.9093(2)	0.0648(1)	0.40379(6)	1.14(2)
C26	0.7318(1)	0.2010(1)	0.38453(6)	1.02(2)
C27	0.8718(1)	0.1662(1)	0.42360(6)	1.00(2)
C28	0.8537(2)	0.1590(1)	0.48826(6)	1.39(2)
O1	0.8538(1)	0.09386(7)	0.22376(4)	1.06(1)
O2	0.8561(1)	0.27817(7)	0.22672(5)	1.15(2)
O3	1.0853(1)	0.18552(8)	0.25825(5)	1.26(2)
Cl1	0.81459(4)	0.46095(3)	0.40734(2)	1.551(6)
Cl2	0.92993(4)	0.49682(2)	0.24811(2)	1.336(5)
Cl3	0.30212(4)	0.06891(3)	0.43479(2)	1.710(6)
OW1	0.3616(1)	0.1267(1)	0.15542(6)	2.01(2)
OW2	0.9039(1)	0.46581(9)	0.07462(5)	1.67(2)
OW3	0.3288(2)	0.0967(1)	0.30315(7)	4.62(3)
OW4	0.3745(2)	0.0406(2)	0.04785(7)	4.33(4)

[a] B_{iso} is defined as one-third of the trace of the orthogonalized B_{ij} tensor.

tions from the anomalous dispersion, were taken from Ref. 21 and used as contained in the programs. The final difference Fourier had extreme points in the range from 1.15 to -0.55 e Å^{-3}. The six largest positive peaks were found in the coordination sphere of the chromium atoms adjacent to the six nitrogen atoms. The final positional parameters of the non hydrogen atoms are listed in Table 5. Anisotropic displacement parameters and positional parameters of the hydrogen atoms and a listing of observed and calculated structure amplitudes are available from the authors.

Magnetic measurements. The Faraday balance used for the magnetic susceptibility measurements has been described elsewhere.[22] The measurements were made at 13 kG field strength.

EPR spectra. All EPR spectra were recorded with a Bruker ESP 300 spectrometer equipped with an Oxford ESR-900 continuous-flow cryostat. The spectra were obtained at X-band (9.37 GHz) using a modulation frequency of 100 kHz and modulation amplitudes between 0.4 and 0.8 mT, and therefore, as usual, appear as first derivatives of absorbtion. The various spectra were recorded from 4 K to room temperature.

UV–VIS spectra were measured on Cary 118c spectrophotometer.

Acknowledgments. We thank Mrs. Solveig Kallesøe Hansen for the magnetic susceptibility measurement and Mr. Flemming Hansen for help with the collection of X-ray diffraction data. We also thank the Danish Natural Science Research Council for its support.

References

1. Wieghart, K., Chaudhuri, P., Nuber, B. and Weiss, J. *Inorg. Chem. 21* (1981) 3086.
2. Wieghart, K., Guttmann, M. and Ventur, D. *Z. Anorg. Allg. Chem. 527* (1985) 33.
3. Andersen, P., Døssing, A. and Pedersen, E. *Acta Chem. Scand., Ser. A 41* (1987) 381.
4. Wieghart, K., Schmidt, W., Endres, H. and Wolfe, C. R. *Chem. Ber. 112* (1979) 2837.
5. Glerup, J., Goodson, P. A. and Hodgson, D. J. *Inorg. Chim. Acta. Submitted.*
6. Andersen, P., Larsen, S. and Pretzmann, U. *Acta Chem. Scand. Submitted.*
7. Glerup, J. *Acta Chem. Scand. 26* (1972) 3775.
8. Glerup, J., Mønsted, O. and Schäffer, C. E. *Inorg. Chem. 15* (1976) 1399.
9. Niemann, A., Bossek, U., Wieghardt, K., Butzlaff, C., Trautwein, A. X. and Nuber, B. *Angew. Chem., Int. Ed. Engl. 31* (1992) 311.
10. Bang, E., Eriksen, J., Glerup, J., Mønsted, L., Mønsted, O. and Weihe, H. *Acta Chem. Scand. 454* (1991) 367.
11. Glerup, J. and Weihe, H. *Acta Chem. Scand. 45* (1991) 444.
12. Kremer, S. *Inorg. Chem. 24* (1985) 887.
13. Andersen, P., Døssing, A., Glerup, J. and Rude, M. *Acta Chem. Scand. 44* (1990) 346.
14. Pedersen, E. and Toftlund, H. *Inorg. Chem. 13* (1974) 1603.
15. Schäffer, C. E. *Structure and Bonding 5* (1968) 67.
16. Thewalt, U. *Z. Anorg. Allg. Chem. 412* (1975) 29.
17. Owen, J. and Harris, E. H. In: Geschwind, S., Ed., *Electron Paramagnetic Resonance*, Plenum Press, New York 1972, p. 427.
18. Kosowsky, W. J. and Bailar, J. C. *J. Am. Chem. Soc. 91* (1969) 3212.
19. Herwig, W. and Zeiss, H. H. *J. Org. Chem. 16* (1977) 2534.
20. SDP
21. *International Tables for X-Ray Crystallography*, Kynoch Press, Birmingham 1974.
22. Josephsen, J. and Pedersen, E. *Inorg. Chem. 16* (1977) 2534.

Received February 9, 1993.